

The Randomly Driven Ising Ferromagnet

Part I:

General Formalism and Mean Field Theory

Johannes Hausmann[†] and Pál Ruján^{†,§}

*Fachbereich 8 Physik[†] and ICBM[§], Postfach 2503, Carl von Ossietzky Universität,
D-26111 Oldenburg, Germany*

(November 18, 2018)

We consider the behavior of an Ising ferromagnet obeying the Glauber dynamics under the influence of a fast switching, random external field. After introducing a general formalism for describing such systems, we consider here the mean-field theory. A novel type of first order phase transition related to spontaneous symmetry breaking and dynamic freezing is found. The non-equilibrium stationary state has a complex structure, which changes as a function of parameters from a singular-continuous distribution with Euclidean or fractal support to an absolutely continuous one. These transitions are reflected in both finite size effects and sample-to-sample fluctuations.

PACS numbers: 05.50+g 05.70.Jk 64.60Cn 68.35.Rh 75.10.H 82.20.M

I. INTRODUCTION

The last decade has seen many advancements in the theory of dynamic systems, both from a mathematically rigorous, as from a physically oriented heuristic point of view. Most of these results have been obtained for systems with few degrees of freedom, attempts at handling nonequilibrium stationary states of systems with macroscopically many degrees of freedom have been made only recently^{1–3}. In this paper we propose a general theoretical framework for *strongly, randomly driven* statistical physical systems and apply it to the Ising model in a random, dichotomic driving external field.

The resulting dynamics has many qualitative similarities with earlier work on one dimensional Ising chains in a binary random field⁴. However, while the ‘dynamics’ defined in⁵ is a one dimensional map generated by the iteration of non-commuting 2×2 transfer matrices, in the present case the map ‘lives’ in 2^N dimensions. Nevertheless, the main mechanism leading to chaotic behavior and strange attractors is in both cases related to the competition between two (or more) fixed points (or limit cycles). In this respect, the randomly driven Ising model (RDIM) has many intriguing aspects which – somewhat unexpectedly – can be handled both analytically and numerically with methods developed earlier for the random field Ising model^{5–11}.

The Ising ferromagnet in a time-dependent sinusoidally oscillating field has received recently a lot of attention, from both a theoretical and experimental point of view. On the theoretical side, Rao, Krishnamurthy, and Pandit¹² have presented a large N -expansion of the cubic $O(N)$ model in three dimensions and calculated the critical exponents related to the area of the hysteresis loop. The underlying dynamic phase transition has been then studied within both mean-field¹³ and Monte Carlo simulations^{14–17}. The theory presented in this paper is a generalization of these ideas for the case when the external field is subject to a chaotic dynamics and/or is a random variable.

Besides the theoretical interest in describing such systems, we believe that many of our predictions can be tested with recently developed experimental techniques. Dynamic magnetization measurements have been recently performed in ultrathin Au(111)/Cu(0001)/Au(111) sandwiches or epitaxial Co/Au(111) films^{18–20}. Similarly, hysteresis measurements on the ultrathin film Co/Au(001)²¹ indicate that below T_c these systems undergo a dynamic phase transition belonging to the Ising-universality class. More relevant to our theory, the time evolution of magnetization clusters can be optically recorded. The typical relaxation times range from minutes to a few seconds with increasing field amplitudes²⁰. This relatively slow relaxation rate allows for a simple experimental realization of the randomly driven external field.

Ultrathin films are potential candidates for magneto-optical storage devices and our approach might be relevant especially in this respect. At well chosen control parameters the stationary magnetization distribution of the RDIM displays several well separated peaks. Thus, when driven appropriately, such materials can store locally more than the two values typical for an equilibrium ferromagnetic system.

This first paper is organized as following: the basic assumptions and the general theoretical formalism are introduced in Section 2. The mean-field theory is presented in full detail in Section 3. In this approximation the paramagnetic–ferromagnetic stationary phase transition becomes first order. The phase boundary is obtained analytically. The average magnetization is non-analytic (jumps) at small driving field values and therefore the usual mean-field approach fails. Nevertheless, the phase transition is related to a spontaneous symmetry breaking and a pitchfork bifurcation of the magnetization distribution. On the other hand, the analytical nature of the stationary magnetization distribution changes from singular continuous with euclidean or fractal support to absolutely continuous along analytically computed boundaries. Such changes are directly connected to finite size effects of the free energy and the multifractal spectrum of the magnetization measure. Close to the para-ferro phase boundary the small magnetization region close to $m \sim 0$ becomes a repeller, inducing ultracritical slowing down related to type-I intermittency. A short summary of the main mean-field features is presented in Section 4.

A subsequent paper considers the randomly driven Ising model in one and two dimensions. Although the one-dimensional case cannot be fully solved, many interesting exact results can be derived. We find a line of second order phase transitions at $T = 0$ between a disordered (driven paramagnetic) and an ordered (ferromagnetic) phase. Along this line the stationary critical exponents change continuously as a function of the driving field strength. However, the dynamic critical exponent remains unchanged, $z = 2$. As a function of temperature and of the driving field strength, the nonequilibrium stationary state might display multifractal or ‘fat’ multifractal character. Hence, the generalized free energy is characterized by anomalous fluctuations related to the existence of a multifractal spectrum. We also performed Monte Carlo simulations on a square lattice. Many features of the mean-field dynamics are shown to survive the strong fluctuations characteristic to two dimensional systems. However, in contrast to the mean-field approach, the two-dimensional model displays also an interesting spatial structure related to droplet dynamics. Comparisons between mean-field theory and two-dimensional results are systematically presented, including some preliminary results for hysteresis.

II. GENERAL FORMALISM

A. The Master Equation

Consider a spin system $\vec{\mu} = (s_1, s_2, \dots, s_N)$ in contact with a thermal bath (phonons). Let us denote by $\tau_{spin-flip}$ the characteristic time of the spin-phonon interactions, and by τ_{sys} the *slowest* relaxation mode of the spin system. For $\tau_{spin-flip} \ll \tau_{sys}$ the system is in *local* thermal equilibrium.

Our basic assumption is that the time evolution of the spin system can be described by a time-dependent joint probability distribution, $P(\{s_i\}; t)$. From a dynamic point of view, one can consider this distribution as an average over all microstate initial conditions satisfying given macroscopic constraints. The rigorous definition of this basic assumption is related to the existence of Markov-partitions in (hyperbolic) dynamic systems^{2,3} and goes beyond the scope of this article.

The distribution $|P(t)\rangle$ obeys the Master Equation:

$$|\dot{P}(t)\rangle = -\hat{\mathcal{L}}_{B(t)}|P(t)\rangle, \quad (1)$$

where the operator $\hat{\mathcal{L}}_{B(t)}$ describes the outflow (inflow) probability from (into) state $\{s_i\}$ into (from) other states, as prescribed by the dynamic rules. The dependence on the field is made explicit because in general $[\hat{\mathcal{L}}_B, \hat{\mathcal{L}}_{B'}] \neq 0$ for $B \neq B'$. Assuming a constant field $B = B_0$ and ordering the eigenvalues of $\hat{\mathcal{L}}_{B_0}$ as $\lambda_0 = 0 \leq |\lambda_1| \leq \dots \leq |\lambda_{2^N-1}|$, one has $\tau_{sys} = |\lambda_1|^{-1}$. The ket vector $|P(t)\rangle$ can be expressed in the spin-configuration basis as $P(\{s_i\}; t)$. Alternately, it can be parameterized as

$$P(\{s_i\}; t) = \frac{1}{2^N} [1 + \sum_{i=1}^N m_i s_i + \sum_{i \neq j} c_{i,j} s_i s_j + \dots] = \frac{1}{2^N} \left(\sum_{\alpha=1}^{2^N} \pi_\alpha \prod_{j \in \alpha} s_j + 1 \right), \quad (2)$$

where the $\pi_\alpha(t)$ are the average values of all possible 2^N products of spins

$$\pi_\alpha(t) = \langle \prod_{j \in \alpha} s_j \rangle = \sum_{\vec{s}} P(\{s_i\}; t) \prod_{j \in \alpha} s_j \quad (3)$$

Hence, $|P(t)\rangle$ can be expressed as a 2^N -dimensional normalized vector in the space of all possible spin configurations, or in the space of spin-products as $\vec{\pi}(t) = (\langle s_1 \rangle, \dots, \langle s_N \rangle, \langle s_1 s_2 \rangle, \dots)$. Note that when expressing the kinetic Ising model Liouville operator in terms of Pauli matrices²² this orthogonal transformation corresponds to the exchange $\sigma^z \leftrightarrow \sigma^x$.

In general, the Liouville operator $\hat{\mathcal{L}}$ is not symmetric but can be expanded in a biorthogonal basis formed by its right, $|r_n\rangle$, and left, $\langle l_n|$, eigenvectors ($\langle l_n | r_m \rangle \sim \delta_{m,n}$):

$$\hat{\mathcal{L}} = \sum_{n=0}^{2^N-1} |r_n\rangle \lambda_n \langle l_n| \quad (4)$$

It is worth noting that since $e^{-\hat{\mathcal{L}}}$ is a stochastic operator, we have $\langle l_0 | \hat{\mathcal{L}} = 0 \langle l_0 |$, where $\langle l_0 | = (1, 1, \dots, 1)$ in the spin-configuration basis. The scalar product $\langle l_0 | r_0 \rangle = Z$ delivers the equilibrium (stationary) canonical partition function.

The time-dependent field $B(t)$ is usually a deterministic one-dimensional map, *e.g.* a harmonically oscillating field. However, if the deterministic map is chaotic, the field becomes a random variable. In what follows we assume that the external field B is a random variable sampled identically and independently from the symmetric distribution $\rho(B) = \rho(-B)$.

Let τ_B be the average sampling time of the field distribution. As long as $\tau_B \gg \tau_{sys}$ the spin system has enough time to relax to global thermal equilibrium. This is the case of equilibrium statistical mechanics and normal fluctuations. The situation can be very different if the field can switch abruptly ($\tau_{switch}^{-1} \sim \mu_B \dot{B}$ is large) and $\tau_{sys} \gg \tau_B$. The system does not have enough time to relax to equilibrium and the stationary state is determined by the external random field. As discussed later, such a situation is experimentally realizable.

Now let us assume that the field is sampled from $\rho(B)$ at time intervals of length τ_B ,

$$B(t) = \mu_B B \rho(B) \sum_{n=0}^{\infty} \Theta(t - n\tau_B) \Theta((n+1)\tau_B - t) \quad (5)$$

We can integrate Eq. (1) exactly from $t_{n-1} = (n-1)\tau_B$ to t for $t_{n-1} < t < t_n$:

$$|P(\{s_i\}; t)\rangle = e^{-\hat{\mathcal{L}}_{B(t_{n-1})}(t-t_{n-1})} |P(\{s_i\}; t_{n-1})\rangle \quad (6)$$

where $B(t_{n-1})$ is the field instance sampled at time t_{n-1} . For $t = \lim_{\epsilon \rightarrow 0}(t_n - \epsilon)$ one obtains

$$|P(\{s_i\}; t_n)\rangle = e^{-\hat{\mathcal{L}}_{B(t_{n-1})}\tau_B} |P(\{s_i\}; t_{n-1})\rangle \quad (7)$$

Since in our case the low lying eigenvalues λ_α of the Liouville operator $\hat{\mathcal{L}}$ satisfy $\lambda_\alpha \tau_B \ll 1$, by expanding the exponential in first order one obtains the discrete ‘coarse grained’ Master Equation

$$\frac{|P(\{s_i\}; t_n)\rangle - |P(\{s_i\}; t_{n-1})\rangle}{\tau_B} = -\hat{\mathcal{L}}_{B(t_{n-1})} |P(\{s_i\}; t_{n-1})\rangle \quad (8)$$

which describes correctly only the long-time behavior of Eq. (1). Short term effects due to the larger eigenvalues of $\hat{\mathcal{L}}$ have already relaxed at the time scale τ_B . This approximated form of the Master Equation is used in all further developments.

One can regard Equation (8) as defining the discrete dynamics governing the probability distribution $|P(\{s_i\}; t_n)\rangle$.

B. The driving field distribution

As already mentioned, the external field might be distributed according to the invariant measure of some chaotic one-dimensional deterministic map. In other applications, the field can be Poisson- or Gauss-distributed. In what follows we restrict ourselves to the binary distribution

$$\rho(B) = \frac{1}{2} \delta(B - B_0) + \frac{1}{2} \delta(B + B_0) \quad (9)$$

Many of our results can easily be generalized to arbitrary continuous distributions. Other results, in particular those concerning the stationary state phase diagram and the critical behavior, depend strongly on the discrete character of the choice (9). Eqs. (8) and (9) map our problem into an iterated function system (IFS)²³. As long as we deal with a finite system of spins, the mathematical results (including the collage theorem) developed by Demko and Barnsley and subsequent work on IFS apply to randomly driven spin models as well. However, from a statistical physical point of view, the interesting things happen *after* taking the thermodynamic limit.

C. The invariant measure

As usual in the theory of dynamic systems, one can ask what is the invariant measure induced by the dynamics (8), see, for example,²⁴. Let $\mathcal{P}_s(\vec{\pi})$ denote the invariant density related to the dynamics Eq. 8. It satisfies the Chapman-Kolmogorov equation:

$$\mathcal{P}_s(\vec{\pi}) = \int d\vec{\pi}' \mathcal{P}_s(\vec{\pi}') \int dB \rho(B) \delta(\vec{\pi} - e^{-\hat{\mathcal{L}}_B \tau_B} \vec{\pi}') \equiv \tilde{\mathcal{K}} \mathcal{P}_s(\vec{\pi}) \quad (10)$$

where $\tilde{\mathcal{K}}$ denotes the Frobenius-Perron (FP) operator. Physically, $\mathcal{P}_s(\vec{\pi})$ describes the nonequilibrium stationary state induced by the Master Equation dynamics. Note that we used above the spin-product basis. An orthonormal transformation of the basis will lead to a different but equivalent FP-operator, the transformation's Jacobian is unity. Again, this is true only for finite systems.

If one is interested in the stationary expectation value of some spin observable $A(\{s_i\})$ one must perform two averages, the 'thermal' $\langle \dots \rangle$ and the 'dynamic' average [...]:

$$\overline{A(\{s_i\})} = [\langle A \rangle] \quad (11)$$

where the 'dynamic' average [...] is taken over \mathcal{P}_s and $\rho(B)$.

The 'thermodynamics' of such driven systems can be computed from the generalized free energy. This is related to the largest Lyapunov exponent Λ of the dynamics as $-\beta\mathcal{F} = \Lambda$. Consider a long dynamic trajectory consisting of $T\tau_B$ sampling points. The Lyapunov exponent is defined as

$$\Lambda = \lim_{T \rightarrow \infty} \frac{1}{T\tau_B} \ln \text{Tr} \left\{ e^{-\hat{\mathcal{L}}_{B(T)} \tau_B} e^{-\hat{\mathcal{L}}_{B(T-1)} \tau_B} \dots e^{-\hat{\mathcal{L}}_{B(1)} \tau_B} \right\} \quad (12)$$

where $B(n) = B(t_n)$ is distributed according to Eq. (9). The same result can be obtained by iterating some general¹ initial unity vector $|p_0\rangle$ as

$$\begin{aligned} |p_1\rangle &= e^{-\hat{\mathcal{L}}_{B(1)} \tau_B} |p_0\rangle, & a_1 &= \sqrt{\langle p_1 | p_1 \rangle} \\ |p_2\rangle &= \frac{1}{a_1} e^{-\hat{\mathcal{L}}_{B(2)} \tau_B} |p_1\rangle, & a_2 &= \sqrt{\langle p_2 | p_2 \rangle} \\ &\dots & & \end{aligned}$$

For large n the vectors $|p_n\rangle$ will be distributed according to \mathcal{P}_s and up to $O(\frac{1}{T})$ corrections the Lyapunov exponent can be expressed as

$$\Lambda = \int d\mathcal{P}_s(\vec{\pi}) \int dB \rho(B) \frac{1}{2} \ln \|e^{-\hat{\mathcal{L}}_B \tau_B} \vec{\pi}\| \quad (13)$$

For a constant field $\rho(B) = \delta(B - B_0)$ and the stationary distribution is $\mathcal{P}_s(\vec{\pi}) = \delta(\vec{\pi} - \vec{\pi}_{eq})$, where $\vec{\pi}_{eq}$ are the Boltzmann-distribution averaged spin-products. Therefore, $\|e^{-\hat{\mathcal{L}}_{B_0} \tau_B} \vec{\pi}_{eq}\| = (\langle l_0 | r_0 \rangle)^2 = Z^2$, where we have used that $\vec{\pi}_{eq}$ is the right eigenvector of $\hat{\mathcal{L}}_{B_0}$ with eigenvalue 0. We recover the usual definition of free energy by multiplying Λ with $-k_B T$.

This generalized free energy might display anomalous fluctuations related to the multifractal spectrum of the stationary distribution \mathcal{P}_s , as will be shown later for the mean field theory.

¹This vector should not fall into any invariant subspace of both $\hat{\mathcal{L}}_{\pm B_0}$ operators

D. Dynamical properties

In order to consider the *dynamical* properties of randomly driven systems one has to solve - in full analogy to the theory of one-dimensional maps - the right eigenvalue problem of the Frobenius-Perron operator:

$$\tilde{\mathcal{K}}\mathcal{R}_m = s_m\mathcal{R}_m \quad (14)$$

The largest magnitude eigenvalue is one, $s_0 = 1$. The right eigenvector \mathcal{R}_0 is nodeless and real: it corresponds to the stationary state, $\mathcal{R}_0 = \mathcal{P}_s$. For $m > 0$ the eigenvectors $\mathcal{R}_m(x)$ satisfy

$$\int d\vec{\pi} R_m(\vec{\pi}) = 0 \quad (15)$$

In addition to the right eigenvectors \mathcal{R}_m , the operator $\tilde{\mathcal{K}}$ might have also a set of null functions of different orders. They correspond to zero eigenvalues of $\tilde{\mathcal{K}}^q$, where q is an integer (the order). These eigenfunctions, however, do not contribute to the relaxation of the initial probability distribution towards \mathcal{P}_s .

In analogy to the usual transfer matrix theory, the relaxation of the probability distribution and of the time dependent correlation functions are determined for asymptotically long times by the second largest eigenvalue s_1 and its eigenfunction \mathcal{R}_1 .

Although at this stage the formalism looks rather involved, it is a straightforward extension of the methods developed for low-dimensional dynamic systems. We consider next the simplest possible example, an Ising model in a random binary external field, Eq. (9). In this case, many interesting stationary and dynamic properties can be obtained analytically, or with numerical methods not more complex than those used for one dimensional maps.

III. MEAN FIELD APPROXIMATION

A. The Mean-Field Map

Consider an Ising model defined on an N -dimensional simplex, such that all spins are nearest neighbors:

$$E = -\frac{J}{N} \sum_{i \neq j} s_i s_j - \mu_B B \sum_i s_i \quad (16)$$

J is normalized so that the energy is additive and μ_B is the Bohr magneton.

Let $\vec{\mu}_i := (s_1, \dots, -s_i, \dots, s_N)$. We may describe the Liouville operator $\hat{\mathcal{L}}$ with the transition rate $w(\vec{\mu}_i|\vec{\mu})$ in the Glauber form²⁵

$$w(\vec{\mu}_i|\vec{\mu}) = \frac{1}{2\alpha} [1 - s_i \tanh(\frac{K}{N} \sum_{j \neq i} s_j + H)] \quad (17)$$

where $\beta = 1/k_B T$, $K = \beta J$, $H = \beta \mu_B B$ and α sets the time constant. Applying Eq. (8) one obtains after performing the thermodynamic limit $N \rightarrow \infty$:

$$m(t+1) = \tanh(Km(t) + H(t)), \quad (18)$$

Time is measured in units of τ_B . The field distribution Eq. (9) leads to the one-dimensional map

$$m(t+1) = \begin{cases} \tanh(Km(t) + H_0) & \text{with probability } \frac{1}{2} \\ \tanh(Km(t) - H_0) & \text{with probability } \frac{1}{2} \end{cases} \quad (19)$$

Note that in the thermodynamic limit the moments of the magnetization do not couple with higher order correlation functions and the methods worked out previously for the one-dimensional random-field Ising chain can thus be applied directly.

Since in the stationary state, Eq. (10), $[m^k(t+1)] = [m^k(t)]$, using Eq. (18) and simple algebraic manipulations we obtain that the k -th moment of the stationary magnetization is given by

$$[m^k] = \left[\left(\frac{v+h}{1+vh} \right)^k \right] \quad k = 1, 2, \dots \quad (20)$$

where $v = \tanh(Km)$ and $h = \tanh(H)$.

At high temperature the system is in the disordered, paramagnetic phase, in which case all odd moments of the magnetization vanish. *Assuming* that the free energy is analytic in $[m]$, the critical temperature is obtained by expanding $[m]$ in first order in $O([h^2])$:

$$[m] \simeq K(1 - h_0^2)[m] \quad (21)$$

and neglecting $[m^q]$, $q = 3$ and higher odd moments (which should scale as $O([h^{2q}])$). In the usual mean-field scenario $[m] = 0$ in the paramagnetic phase and the coefficient vanishes at the transition point to the ferromagnetic phase:

$$H_c^{(II)} = \frac{1}{2} \ln \frac{1+m^\dagger}{1-m^\dagger}, \quad (22)$$

where $m^\dagger = \pm \sqrt{\frac{K-1}{K}}$ for $K > 1$. Using a simple geometric argument we will show below that this analyticity assumption fails and the phase transition is actually first order. For the second moment one obtains

$$[m^2] \simeq \frac{h_0^2}{1 - K^2(1 - 4h_0^2 + 3h_0^4)} \quad (23)$$

where we have omitted $O([m^4])$ and higher even moments. The pole of this expression is also related to the phase transition, which is discussed below. Third and fourth order expansions of $[m]$ and $[m^2]$ read

$$[m] \simeq \left(K(1 - h_0^2) - \frac{K^4(h_0^2 - h_0^4)}{1 - K^3(1 - 10h_0^2 + 19h_0^4 - 10h_0^6)} \right) [m] \quad (24)$$

and

$$[m^2] \simeq \left(h_0^2 - \frac{h_0^4 K^4 (2 - 17h_0^2 + 30h_0^4 - 15h_0^6)}{3 - K^4(3 - 60h_0^2 + 212h_0^4 - 260h_0^6 + 105h_0^8)} \right) \times \left(1 - K^2(1 - 4h_0^2 + 3h_0^4) + \frac{K^6(2 - 17h_0^2 + 30h_0^4 - 15h_0^6)(6h_0^2 - 16h_0^4 + 10h_0^6)}{3 - K^4(3 - 60h_0^2 + 212h_0^4 - 260h_0^6 + 105h_0^8)} \right)^{-1} \quad (25)$$

respectively. A high order expansion of the moments along these lines can be easily obtained using algebraic manipulations programs but will not be presented here.

B. The stationary phase diagram

In principle, there are at least two different mechanisms for a phase transitions in the stationary state described by $\mathcal{P}_s(m)$. The first one corresponds to spontaneous symmetry breaking leading to a continuous phase transition. In this scenario the stationary distribution, which at high temperature is a function of the even magnetization moments only, $\mathcal{P}_s(m) = \mathcal{P}_s(-m)$, becomes degenerate at certain parameter values $\{K, H_0\}$ and the odd subspace, $\mathcal{P}_o(m) = -\mathcal{P}_o(-m)$, contributes as well. More precisely, $\mathcal{P}_s(m) = \mathcal{R}_0$ is **always** a nodeless even function of m . The field symmetry is spontaneously broken when the largest odd-subspace eigenvalue of the Frobenius-Perron operator Eq. (14), $s_1 \rightarrow 1$. Therefore, the largest eigenvalue is degenerate and the corresponding eigenvector is an arbitrary linear combination of $\mathcal{P}_s(m)$ and $\mathcal{R}_1(m) = -\mathcal{R}_1(-m)$, leading to a non-vanishing order parameter. Close to but above the transition point the relaxation time of the stationary distribution diverges as $\tau^{-1} \sim 1 - s_1$. We find no evidence for such a mechanism, at least not in mean-field approximation. Instead, the phase transition is related to a bifurcation of the stationary magnetization distribution.

Consider the map Eq. (19) at high temperature, a situation shown in Fig. 1. The arrows indicate the direction of the flow. The competition between the two stable fixed points leads to chaotic behavior and the displayed stationary distribution. To approximate the distribution, we tracked the evolution of 1000 (random) initial values of m subject to the map for 1000 iterations. At low temperatures ($K > 1$) and large fields one has the situation depicted in Fig. 2. Note the possible intermittent behavior close to $m \sim 0$. If we decrease H_0 the map can ‘pinch’ tangentially the $m(t+1) = m(t)$ diagonal, creating thus one new unstable fixed point. This situation is shown in Fig. 3. Decreasing the field even further, we have the map of Fig. 4, where \mathcal{P}_s has bifurcated into two stable and one unstable disjoint distributions. For further use let us denote by m_1 , m_2 , and m_3 the possible fixed points of the equation $m = \tanh(Km + H_0)$ in descending order. The line of the critical field H_c can be calculated from the condition that at the new fixed point the map is tangential (‘critical map’, see²⁶) and leads after elementary calculations to

$$H_c = \frac{1}{2} \ln \frac{1 - m^\dagger}{1 + m^\dagger} + Km^\dagger \quad (26)$$

where $m^\dagger = m_2 = m_3$.

From Figs. 2-4 it is evident that $|m| > m^\dagger$ and except for $H_0 = 0$ the magnetization jumps at the phase transition. We believe that this feature is due to the discrete character of the binary $\rho(B)$ distribution. Thus, the RDIM provides an example of a spontaneous symmetry breaking leading to a first order phase transition. The mechanism behind this first order transition is very different from that of equilibrium systems and is related to a tangential bifurcation of the stationary distribution. The corresponding phase diagram is shown in the upper part of Fig. 5.

C. The multifractal regime

Some highly unusual properties of the RDIM are related to the multifractal spectrum of the stationary state. Following the notation introduced in²⁷, one can identify a singular-continuous density with fractal support (SC-F) in both the paramagnetic and the ferromagnetic phase. When a gap opens between the upper and the lower branch of the map the invariant distribution has a fractal support with the capacity dimension $d_0 < 1$. The border of the (SC-F) region is given by $Km_1 = H_0$ in

the para- and $K(m_1 + m_3) = 2H_0$ in the ferromagnetic phase. In the region between $d_0 = 1$ and $d_\infty = 1_-$ the distribution is singular-continuous with Euclidean support (SC-E)²⁷. Using the ideas developed in⁶, we obtain $d_\infty = 1$ if $K(1 - m_1^2) = \frac{1}{2}$. The density distribution is absolutely continuous (AC) if all generalized dimensions²⁸ equal one, $d_q = 1$, ($q = 0, \dots, \infty$). These results are graphically summarized in the lower part of Fig. 5.

In order to compute the generalized free energy, Eq. (13), one can use that $\langle l_0 | r_n \rangle = \delta_{0,n} \sum_{\{s_i\}} P_{eq}(\{s_i\})$. Note that the left eigenvector $\langle l_0 |$ of the $\hat{\mathcal{L}}_B$ operator corresponds to a sum over all spin configurations and is therefore independent of B . When inserting in the product within the trace of Eq. (12) the spectral decompositions of different non-commuting operators $\hat{\mathcal{L}}_B$, the ground state contributions decouple from the higher level contributions. Hence, in mean field approximation the free energy is given as expected by

$$-\beta\mathcal{F} = N \int dm \mathcal{P}_s(m) \frac{1}{2} \ln 2 [\cosh(2Km) + \cosh(2H_0)] \quad (27)$$

This integral can be approximated above H_c by expanding the integrand in even moments of the magnetization (see Eq. (23) and (25)). The fluctuations of the free energy depend on the (multifractal) structure of the stationary $\mathcal{P}_s(m)$ distribution.

Strictly speaking, Eq. (27) is the average free energy. When considering a finite system or a long but finite dynamic trajectory, the free energy is normally distributed. As shown in⁸ for the one dimensional random field Ising model, in the SC-F region the multifractal spectrum can be directly related to the second cumulant of the free energy distribution. The arguments presented in⁸ apply also to our case, a broad multifractal distribution leads to large free energy fluctuations.

In the SC-F regime one can obtain additional information about finite-size free-energy fluctuations from the generalized dimensions (Legendre-transform of the multifractal spectrum). We applied the methods developed in^{6-8,11,29} and computed numerically the multifractal spectrum of the stationary distribution.

Another interesting observation is that these isolines cannot directly cross into the ferromagnetic region: close but above the phase transition there is no positive gap (see Figs. 2-3). Nevertheless, in the ferromagnetic phase the magnetization distribution itself can be multifractal. This is shown in Fig 4. The inset shows the enlarged part of the map leading to a multifractal distribution for positive magnetization (a symmetric counterpart exists for negative magnetization).

D. Dynamical properties

The stationary phase transition at H_c , Eq. (26), is from a physical point of view a **dynamic freezing** transition characterized by an extremely slow dynamics. As shown below, the relaxation of the map - and hence of all time-dependent correlation functions - diverges exponentially fast close to the critical field H_c . Consider first the mean-field map close but above the critical field, as illustrated in Fig. 6.

The iteration along the upper branch alone corresponds to type I intermittency and has been discussed previously in the theory of chaotic maps^{26,30,31}. As usual, the function $m' = \tanh(Km + H_0)$ will be approximated up to quadratic order close to the point (m^\dagger, H_c) where $m^\dagger = \pm \sqrt{\frac{K-1}{K}}$ is the point where the upper branch touches tangentially the $m' = m$ line. Introducing the new variable $x = \frac{m-m^\dagger}{K(1-m^{\dagger 2})}$, one obtains

$$x_{n+1} = x_n + m^\dagger x_n^2 + \frac{H_0 - H_c}{K} \quad (28)$$

Requiring that $\frac{x_{n+1}-x_n}{\delta n}$, x^2 , and $\frac{H_0-H_c}{K}$ have the same order of magnitude implies that δn and hence n must scale as

$$n \sim \left(\frac{H_0 - H_c}{K} \right)^{-\frac{1}{2}} \quad (29)$$

which is the standard result for one-dimensional maps²⁶.

However, the probability to stay on the upper branch of the map for n consecutive steps is exponentially small. Assume that at time $t = 0$ one injects N_0 points at the $m = -1$ location. In order to move upwards, the points can use only the upper branch and must pass through the ‘intermittent tunnel’. Once a trajectory flips to the lower branch, it is set back to the entrance of the tunnel. If a point has passed through the tunnel, it might eventually return to the lower part but has a similar chance of being trapped on the symmetric upper part. This dynamics can be modeled by the Markov process shown in Fig. 7.

By iterating the corresponding stochastic matrix (or by full induction) it is easy to see that the stationary probability of being at site n is given by $p_n = \frac{1}{2^n}$. Therefore, assuming quasi equilibrium, the escape rate is estimated as

$$\dot{N}(t) = -\frac{a}{2^n} N(t) \quad (30)$$

where a is a constant of order $O(1)$ related to the probability of return after escape. The relaxation time τ corresponding to Eq. (30) diverges as

$$\tau = \frac{2^n}{a} \sim 2^{\alpha[H_0-H_c]} \quad (31)$$

where we have used Eq. (29), α is a constant. Hence, the relaxation time diverges exponentially fast close to the phase transition. Below H_c , the slow dynamics is due to the average escape time (fractal dimension) from the central repeller.

Another interesting dynamic phenomenon is the hysteresis of the RDIM. Here one adds a harmonic part to the external driving field:

$$H(t) \mapsto H(t) + A \cos \Omega t \quad (32)$$

The resulting hysteresis distribution is shown in Fig. 8. The evolution of 500 initial values was tracked for 2000 iterations. We close here the discussion of the mean-field (or infinite dimensional) RDIM. We expect many of the features discussed here to be valid in three dimensional systems and to a lesser extent in two dimensions.

IV. SUMMARY AND DISCUSSION

In this paper we have discussed the behavior of a spin system with short range interactions in a random external field coupled to the order parameter. If the distribution of the external field is discrete, the resulting dynamics is chaotic due to the competition between different equilibrium states of the system. We proposed a general formalism for calculating the stationary and dynamical properties of randomly driven systems and applied it to the Ising model. In the mean-field approximation the stationary distribution of the magnetization displays a spontaneous symmetry breaking phase at low fields and temperatures. The transition between the disordered and the ferromagnetic phase is first order and corresponds to a tangential bifurcation of the underlying map. Close to the phase transition the characteristic relaxation time diverges *exponentially* - leading to dynamic freezing. Depending on

the control parameters, the stationary magnetization distribution can be a normal, multifractal or fat-fractal distribution in both the disordered and ordered phases.

Our interest in this problem arises mainly in connection to understanding the nature of open systems with many degrees of freedom. Information processing systems, natural or artificial, have a macroscopic number of connected elements subject to external stimuli changing faster than the characteristic thermal relaxation time. As illustrated by the simple example presented in this paper, such systems might develop stationary states far from equilibrium which might be many times more effective in dynamically storing information than simple thermal equilibrium states. In this respect it would be also of interest to consider other choices for the driving field distribution. Continuous distributions, for instance, might lead to very different stationary phase transitions than the one discussed here.

In “The randomly driven Ising ferromagnet”, Part II, we discuss the RDIM in one and two dimensions.

ACKNOWLEDGEMENTS

This article was initiated during PR’s visit at the Hong Kong University of Science and Technology. PR thanks the staff of the Department of Physics and in particular N. Cue, K.Y. Szeto, and M. Wong for their warm hospitality. This work was partly supported by the DFG through SFB 517.

- ¹ N. Simányi and D. Szász, The Boltzmann-Sinai hypothesis for hard ball systems, preprint, *mp-arc.math.utexas.edu* - #95-133
- ² G. Gallavotti and E. G. D. Cohen, Dynamical ensembles in nonequilibrium statistical mechanics, *Phys. Rev. Lett.* **74** (1995) 2694
- ³ G. Gallavotti and E. G. D. Cohen, Dynamical ensembles in stationary states, *J. Stat. Phys.* **80** (1995) 931
- ⁴ R. Bruinsma and G. Aeppli, One dimensional Ising model in a random field, *Phys. Rev. Lett.* **50** (1983) 1494
G. Aeppli and R. Bruinsma, Linear response theory and the one-dimensional Ising ferromagnet in a random field, *Phys. Lett. A* **97** (1983) 117
- ⁵ G. Györgyi and P. Ruján, Strange attractors in disordered systems, *J. Phys. C* **17** (1984) 4207
- ⁶ S. N. Evangelou, Fractal measures in the random-field Ising model, *J. Phys. C* **20** (1987) L511
- ⁷ P. Szépfalussy and U. Behn, Calculation of a characteristic fractal dimension in the one-dimensional random Ising model, *Z. Phys. B* **65** (1987) 337
- ⁸ J. Bene and P. Szépfalussy, Multifractal properties in the one-dimensional random-field Ising model, *Phys. Rev. A* **37** (1988) 1703
- ⁹ U. Behn and V. A. Zagrebnov, One-dimensional Markovian-field Ising model: Physical properties and characteristics of the discrete stochastic mapping, *J. Phys. A* **21** (1987) 2151
- ¹⁰ U. Behn and V. A. Zagrebnov, One-Dimensional Random Field Ising Model and Discrete Stochastic Mappings, *J. Stat. Phys.* **47** (1987) 939
- ¹¹ J. Bene, Multifractal properties of a class of non-natural measures as an eigenvalue problem, *Phys. Rev. A* **39** (1989) 2090
- ¹² M. Rao, H. R. Krishnamurthy, and R. Pandit, Magnetic hysteresis in two spin systems, *Phys. Rev. B* **42** (1990) 856

- ¹³ T. Tomé and M. J. de Oliveira, Dynamic phase transition in the kinetic Ising model under a time-dependent oscillating field, *Phys. Rev. A* **41** (1990) 4251
- ¹⁴ W. S. Lo and R. A. Pelcovits, Ising model in a time-dependent magnetic field, *Phys. Rev. A* **42** (1990) 7471
- ¹⁵ S. Sengupta, Y. Marathe, and S. Puri, Cell-dynamic simulation of magnetic hysteresis in two-dimensional Ising system, *Phys. Rev. B* **45** (1992) 7828
- ¹⁶ P. A. Rikvold, H. Tomita, S. Miyashita, and S. W. Sides, Metastable lifetimes in a kinetic Ising model: dependence on field and system size, *Phys. Rev. E* **49** (1994) 5080
- ¹⁷ S. W. Sides, R. A. Ramos, P. A. Rikvold, and M. A. Novotny, Response of kinetic Ising model system to oscillating external fields: Amplitude and frequency dependence, *J. Appl. Phys.* **79** (1996) 6482
- ¹⁸ G. Bayreuther, P. Bruno, G. Lugert, and C. Turtur, Magnetic aftereffect in ultrathin ferromagnetic films, *Phys. Rev. B* **40** (1989) 7399
- ¹⁹ J. Pommier, P. Meyer, G. Pénissard, J. Ferré, P. Bruno, and D. Renard, Magnetization reversal in ultrathin ferromagnetic films with perpendicular anisotropy: domain observations, *Phys. Rev. Lett.* **65** (1990) 2054
- ²⁰ R. Allensbach, M. Stampanoni, and A. Bischof, Magnetic domains in thin epitaxial Co/Au(111) films, *Phys. Rev. Lett.* **65** (1990) 3344
- ²¹ Y.-L. He and G.-C. Wang, Observation of dynamic scaling of magnetic hysteresis in ultrathin ferromagnetic Fe/Au(001) films, *Phys. Rev. Lett.* **70** (1993) 2336
- ²² B. U. Felderhof, *Rep. Math. Phys.* **1** (1970) 1
E. D. Siggia, Pseudospin formulation of kinetic Ising models, *Phys. Rev. B* **16** (1977) 2319
- ²³ M. F. Barnsley and S. Demko, Iterated function systems and the global construction of fractals *Proc. R. Soc. Lond. A* **399** 243 (1985)
- ²⁴ S.-J. Chang and J. Wright, Transitions and distribution functions for chaotic systems, *Phys. Rev. A* **23** (1981) 1419
- ²⁵ R. J. Glauber, Time-dependent statistics of the Ising model, *J. Math. Phys.* **4** (1963) 294
- ²⁶ Y. Pomeau and P. Manneville, Intermittent transition to turbulence in dissipative dynamic systems, *Commun. Math. Phys.* **74** (1980) 189
- ²⁷ G. Radons, A new transition for projections of multifractal measures and random maps, *J. Stat. Phys.* **72**, 227 (1993)
- ²⁸ H.G.E. Henshel and I. Procaccia, *Physica D* **8**, 435 (1983)
- ²⁹ K. Y. Tsang, Dimensionality of strange attractors determined analytically, *Phys. Rev. Lett.* **57** (1986) 1390
C. Tang and M. Kohmoto, Global scaling properties of the spectrum for a quasiperiodic Schrödinger equation, *Phys. Rev. B* **34** (1986) 2041
- ³⁰ S. Grossmann and H. Horner, Long time tail correlations in discrete chaotic dynamics, *Z. Phys. B* **60** (1985) 79
- ³¹ G. Györgyi and P. Szépfalusy, Relaxation processes in chaotic states of one dimensional maps, *Acta Phys. Hun.* **64** (1988) 33

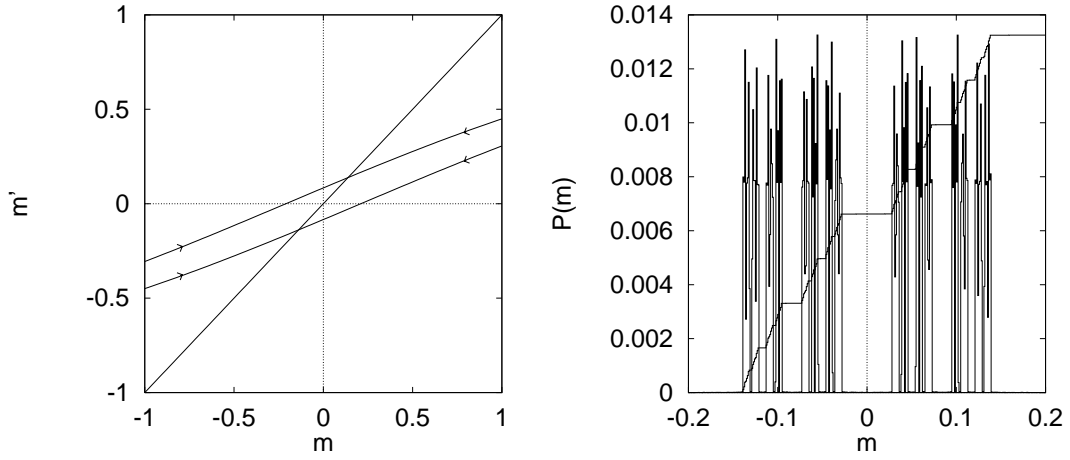


FIG. 1. Mean field map and the stationary distribution in the paramagnetic phase ($K = 0.4$ and $H_0/K = 0.21$).

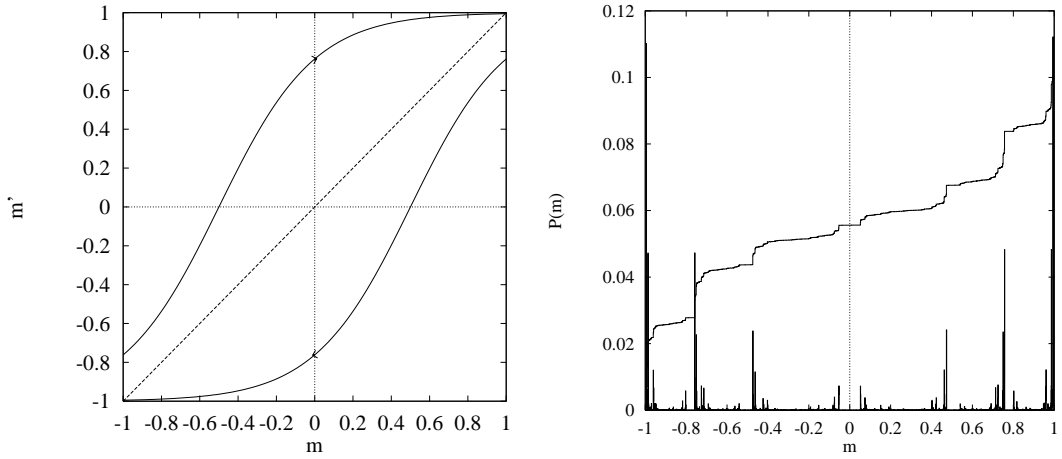


FIG. 2. Mean field map and the stationary distribution for $K = 2.0$ and $H_0/K = 0.5$. The map shows that for strong driving fields the system remains in the paramagnetic phase even below the equilibrium critical temperature.

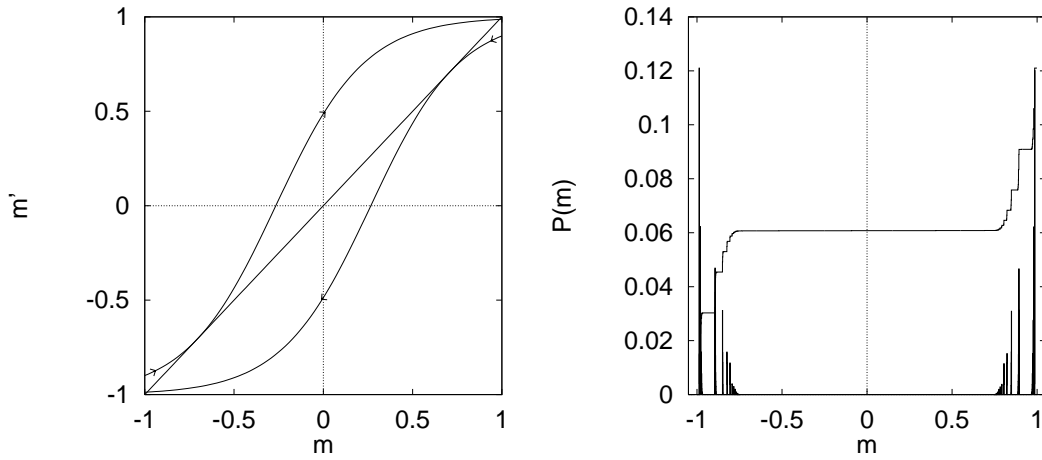


FIG. 3. Same as in Fig. 1 but close to the critical field value ($K = 2.0$ and $H_0/K = 0.266$). Two disjoint distributions are created around the stable fixed points, a repeller in the middle.

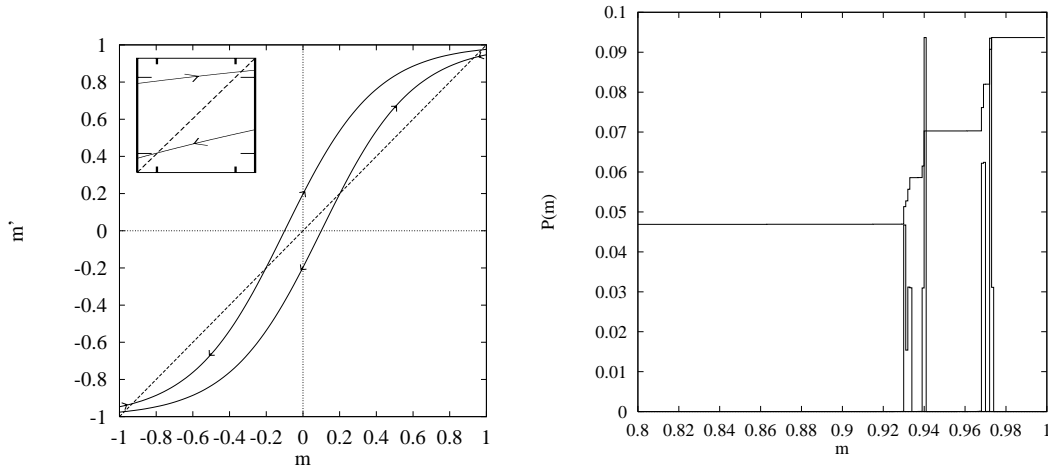


FIG. 4. Mean field map and the stationary distribution in the ferromagnetic phase ($K = 2.0$ and $H_0/K = 0.1$).

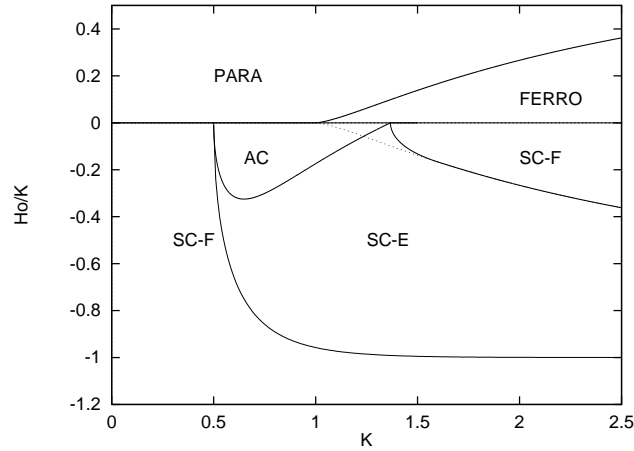


FIG. 5. Mean field phase diagram. The upper part ($H_0 > 0$) shows the border between the para- and ferromagnetic phase. In the lower part ($H_0 < 0$) the regions denoted by SC-F, SC-E correspond to a singular-continuous invariant density with fractal and Euclidean support, respectively, while in the AC-region the density is absolutely-continuous. Note that the diagram is actually symmetric in H_0 .

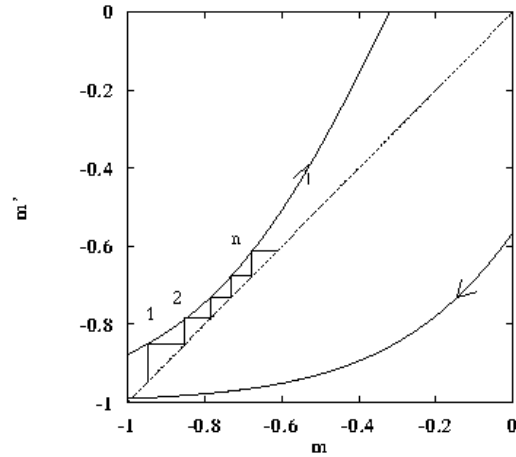


FIG. 6. Lower part of the mean field map for $H \geq H_c$. Iteration along the upper branch is type I intermittent while the lower branch brings the iteration to the starting point in one step.

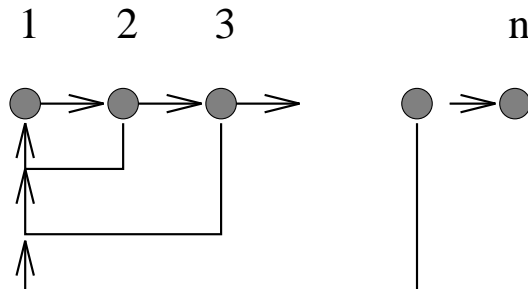


FIG. 7. The Markov process representing the passage through an intermittent tunnel. Each arrow indicates a transition probability of $\frac{1}{2}$.

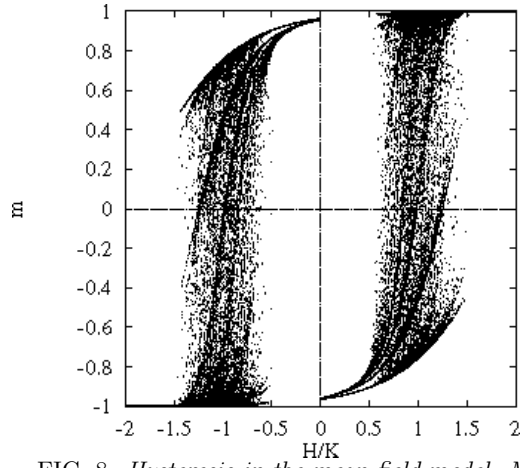


FIG. 8. *Hysteresis in the mean field model. Magnetization $m(t)$ vs. the external driving field $H(t)$, see Eq. (32), for parameters $\frac{A}{K} = \frac{H_0}{K} = 1$, $K = 2$, and $\Omega = \frac{2\pi}{1000}$.*